

Far-infrared investigation of the pseudogap in underdoped $\text{Pb}_2\text{Sr}_2(\text{Y/Ca})\text{Cu}_3\text{O}_8$

M. Reedyk

Department of Physics, Brock University, St. Catharines, Ontario, Canada L2S 3A1

T. Timusk

Department of Physics and Astronomy, McMaster University, Hamilton, Ontario, Canada L2S 4M1

Y.-W. Hsueh and B. W. Statt

Department of Physics, University of Toronto, Toronto, Ontario, Canada M5S 1A7

J. S. Xue* and J. E. Greedan

Department of Chemistry and Brockhouse Institute for Materials Research, McMaster University, Hamilton, Ontario, Canada L2S 4M1

(Received 13 March 1997)

The optical conductivity of underdoped $\text{Pb}_2\text{Sr}_2(\text{Y/Ca})\text{Cu}_3\text{O}_8$ has been obtained from 40 to 700 cm^{-1} via Kramers-Kronig analysis of the c -axis-polarized reflectance measured at temperatures between 10 and 300 K. In the normal state at the lowest and highest frequencies where it is least obscured by a large phonon contribution, the background c -axis optical conductivity of underdoped $\text{Pb}_2\text{Sr}_2(\text{Y/Ca})\text{Cu}_3\text{O}_8$ is observed to decrease systematically as the temperature is lowered from 300 to near 150 K. Upon lowering the temperature further, the optical conductivity remains constant until the superconducting transition temperature of 65 K is reached, whereupon, at the lowest frequencies only, a further depression is observed due to the removal of spectral weight into the superconducting condensate. The spectral weight which is redistributed into the δ -function condensate is estimated to derive from frequencies below 425 cm^{-1} . The depressed conductivity in the normal state is attributed to the formation of a pseudogap similar to that previously observed for underdoped $\text{YBa}_2\text{Cu}_3\text{O}_{7-y}$, $\text{YBa}_2\text{Cu}_4\text{O}_8$, and $\text{La}_{2-x}\text{Sr}_x\text{CuO}_4$. The temperature dependence suggests that the pseudogap is fully formed at a temperature of the order 150 K. This corresponds closely to the temperature range where a change in slope of the ab -plane dc resistivity, and a decrease in the ^{63}Cu NMR Knight shift are observed. [S0163-1829(97)05037-6]

I. INTRODUCTION

The unconventional, and highly anisotropic response of the high- T_c superconductors in the far-infrared region of the electromagnetic spectrum has been well documented, and much discussed.¹ From the time single-crystal samples were available the main focus has been on understanding the transport within the CuO_2 planes. This is primarily the consequence of the fact that the superconductivity is believed to originate within these quasi-two-dimensional sheets, but also because the actual physical geometry of the single-crystal samples in most cases dictates that measurements along the c direction will be difficult due to the small dimension. Nevertheless, a growing body of work aimed at examining the transport along the c axis has been developing, and has yielded interesting results.²⁻⁷ One of the most significant is the observation of the formation of a pseudogap in the low and essentially frequency-independent normal-state optical conductivity as the temperature is lowered below a characteristic temperature, typically significantly higher than the superconducting transition temperature.² The pseudogap gives rise to a non-Drude semiconductinglike c -axis dc resistivity in underdoped materials.⁸ The opening of the pseudogap in the spectrum of low-energy excitations can also be observed in nuclear magnetic resonance (NMR),⁹ specific-heat,¹⁰ and neutron-scattering experiments.¹¹ Its influence on the transport properties is not limited to the c

direction. It has been shown to affect the in-plane dc resistivity,¹² as well as the in-plane frequency-dependent scattering rate.^{13,14}

The pseudogap has been clearly observed in the low-frequency c -axis optical conductivity of underdoped $\text{YBa}_2\text{Cu}_3\text{O}_{7-x}$ with $x \approx 0.3$,² and $\text{YBa}_2\text{Cu}_4\text{O}_8$ which is naturally underdoped.⁴ Both of these materials have double CuO_2 layers, and in both cases the conductivity is depressed at low temperatures below a well-defined pseudogap edge near 300 cm^{-1} . For the single layer material, $\text{La}_{2-x}\text{Sr}_x\text{CuO}_4$, the results are somewhat less clear. Uchida *et al.* found a weak pseudogap behavior in the normal state for an underdoped sample with $x=0.12$, at frequencies below 650 cm^{-1} ,⁵ while Basov *et al.* found for a sample with $x=0.15$ that, while the conductivity is depressed in the far infrared as the temperature is lowered, there was no clear low-frequency signature of the pseudogap edge, and that in fact the energy scale for this non-Drude-like behavior extends to 0.5 eV.⁶ The depressed conductivity associated with the pseudogap thus seems to be a general property of the underdoped cuprate superconductors however its energy scale appears to be somewhat material dependent. Despite observed material-specific differences in the manifestation of the pseudogap Basov *et al.* noted that the superconducting state behavior is quite similar across the various families of compounds. That is, in both one- and two-layer materials there is a further depression in the *low-frequency* optical conductivity below

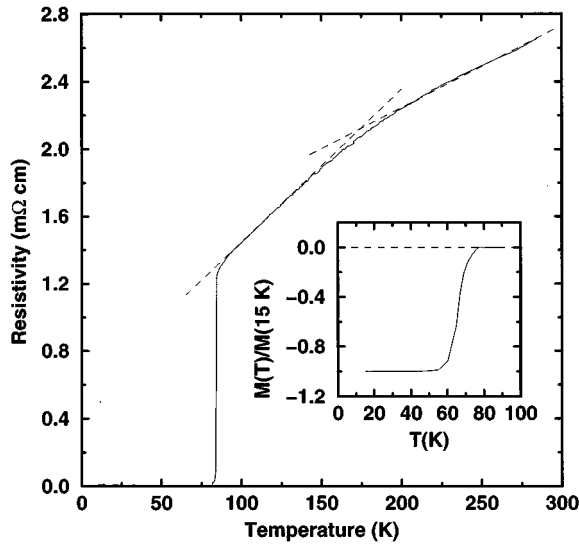


FIG. 1. In-plane dc resistivity (solid curve) of underdoped $\text{Pb}_2\text{Sr}_2(\text{Y}/\text{Ca})\text{Cu}_3\text{O}_8$ (main figure). Note, with the aid of the dashed lines, the change in slope which occurs between 150 and 200 K. Although the dc resistivity indicates zero resistance is attained at 80 K, the magnetization as shown in the inset, suggests that bulk superconductivity occurs near 65 K (the midpoint of the magnetic transition).

T_c which can be accounted for by the formation of the superfluid condensate.⁶ In order to further generalize these observations it is necessary to examine the nature of the pseudogap in other materials. In what follows we report our results of a study of the pseudogap in the c -axis optical conductivity of the underdoped $\text{Pb}_2\text{Sr}_2(\text{Y}/\text{Ca})\text{Cu}_3\text{O}_8$ system.

II. EXPERIMENTAL DETAILS AND SAMPLE CHARACTERIZATION

Single-crystal samples of underdoped $\text{Pb}_2\text{Sr}_2(\text{Y}/\text{Ca})\text{Cu}_3\text{O}_8$ were synthesized using a PbO/NaCl flux technique described previously.¹⁵ For representative crystals, the ab -plane dc resistivity measured in a van der Pauw geometry, and the magnetization measured using a Quantum Design superconducting quantum interference device magnetometer, are shown in the main panel, and the inset to Fig. 1 respectively. As a result of the reduced carrier density, the magnitude of the dc resistivity of the underdoped crystal is, as expected, greater than that of more optimally doped samples.¹⁶ Although the superconducting transition temperature, as determined from the dc resistivity, appears to be 80 K, the magnetization data suggests that the situation is more complicated. The magnetization curve indicates that while the onset of superconductivity occurs near 80 K, that true bulk superconductivity, often defined to occur at the midpoint of the transition, does not appear for the underdoped crystal until approximately 65 K. In optimally doped samples the magnetic transition is much sharper.³ As discussed below, the optical data further support the conclusion that for underdoped $\text{Pb}_2\text{Sr}_2(\text{Y}/\text{Ca})\text{Cu}_3\text{O}_8$ bulk superconductivity has a lower onset.

The method employed for the reflectance measurement makes use of an overfilled sample mounted on a light-scattering cone and an *in situ* gold evaporation to account for

irregularities in sample shape and surface morphology.¹⁷ The ac face, measuring approximately $300 \mu\text{m}$ by $600 \mu\text{m}$ (where the smaller dimension is along c), of a single crystal was used. All measurements were carried out in an s -polarized geometry. It was necessary to mechanically polish the rough face of this submillimeter sized crystal to obtain a measurable signal. The c -axis measurements were carried out using a Michelson-type rapid scan interferometer in the range from 40 to 700cm^{-1} at temperatures between 10 and 300 K. High-frequency extensions for the Kramers-Krönig analysis were obtained as described previously.³

The optical data are compared with results from NMR measurements on crystals from the same synthesis batch. Standard pulsed NMR techniques were used in a field of $H_0 \approx 7.8 \text{ T}$ to measure the Knight shift of the planar $\text{Cu}(2)$ atoms. The sample was a composite of 29 crystals aligned on a quartz plate, held in place with vacuum grease. The $\text{Cu}(2)$ signal is readily distinguished from the $\text{Cu}(1)$ signal ($\text{Cu}(1)$ sites lie between the PbO planes) which has a spin-lattice relaxation rate four orders of magnitude less than that of the $\text{Cu}(2)$ sites.

III. RESULTS

The Kramers-Krönig derived optical conductivity, $\sigma_1(\omega)$, is shown in Fig. 2. Figure 2(a) shows $\sigma_1(\omega)$ for temperatures between 300 and 135 K. Since the evolution of the phonon features with doping and with temperature has been examined in detail in a previous study,³ and since they are not particularly relevant to the discussion that follows, the phonons have been cutoff in the figure. Note that the electronic background at both high frequencies above the range of the phonons and at low frequencies below the range of the phonons appears to decrease monotonically with decreasing temperature. Figure 2(b) shows the optical conductivity at temperatures between 135 and 65 K. In this temperature range the background conductivity remains constant. Figure 2(c) shows the optical conductivity as the sample enters the superconducting state. Note that there is a further decrease in the low-frequency background conductivity (as well as significant changes in the phonon features as discussed previously³).

In Figs. 3(a) and 3(b) we summarize the temperature dependence of the optical conductivity at 700 and 50cm^{-1} , above and below the range of the phonons, respectively. It is clear that its behavior can be divided into three regimes, with the crossover between the high- and intermediate-temperature regimes occurring near 150 K. The low-temperature regime, which is only evident in the low-frequency data of (b), corresponds to temperatures in the superconducting state. In Fig. 3(c) we show for comparison the temperature dependence of the spin component of the planar ^{63}Cu Knight shift with the magnetic field oriented perpendicular to the c axis of the crystals. A temperature-independent orbital component has been subtracted. The temperature dependence can also be characterized by three distinct temperature regimes with similar crossover temperatures.

IV. DISCUSSION

The first point to be made upon examination of Fig. 2 is that unlike the other two-layer materials, $\text{YBa}_2\text{Cu}_3\text{O}_7$ and

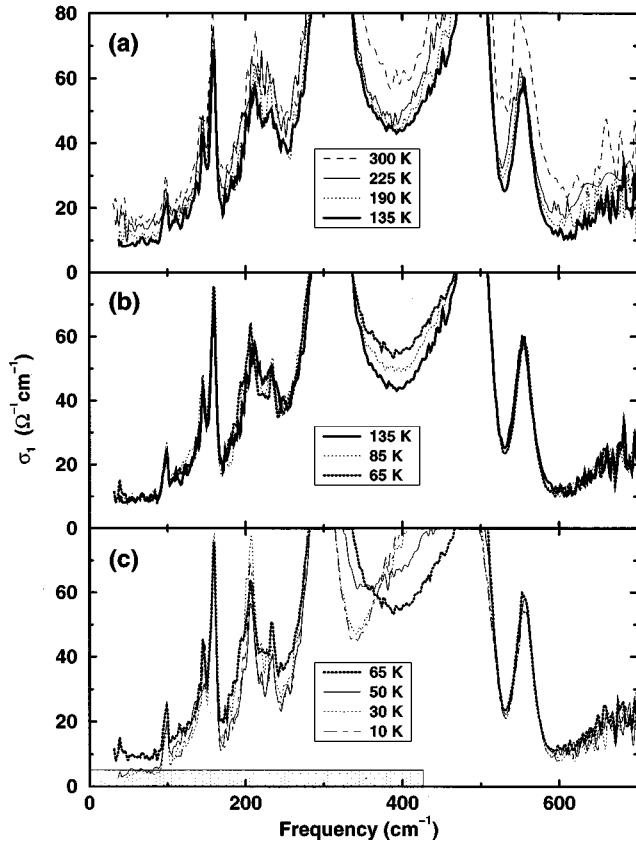


FIG. 2. c -axis-polarized real optical conductivity of underdoped $\text{Pb}_2\text{Sr}_2(\text{Y}/\text{Ca})\text{Cu}_3\text{O}_8$. The upper panel (a) shows the temperature dependence observed between 300 and 135 K. Note that the low background conductivity upon which the strong phonons sit decreases monotonically with decreasing temperature. The middle panel (b) shows $\sigma_1(\omega)$ at temperatures between 135 K and $T_c = 65$ K. Note that the background conductivity remains constant. The lower panel (c) shows $\sigma_1(\omega)$ upon entry to the superconducting state. Note that at low frequencies the background conductivity is suppressed, while at high frequencies it remains constant. The shaded horizontal bar corresponds to the spectral weight of the superconducting condensate.

$\text{YBa}_2\text{Cu}_4\text{O}_8$ for which c -axis optical conductivity data are available, there is no observable sharp pseudogap edge in the low-frequency far-infrared data for underdoped $\text{Pb}_2\text{Sr}_2(\text{Y}/\text{Ca})\text{Cu}_3\text{O}_8$. It is conceivable, but unlikely given the discussion that follows, that such a feature could be hidden underneath the large phonon structure. Efforts to subtract the phonons in order to extract the background conductivity were found to be extremely susceptible to the choice of its shape in the fitting procedure. That is, due to the asymmetric line shape of the phonons, and their large oscillator strength relative to the background conductivity, a smooth background with no sharp features yielded an equally good fit for the normal-state conductivity as a background in the form of a broadened step function. Nonetheless, the data of Figs. 2 and 3 clearly show that there is a depression of the c -axis far-infrared optical conductivity, at both low and high frequencies as the temperature is lowered from 300 to 150 K, to approximately half of its room-temperature value, an observation consistent with the existence of a pseudogap with an energy scale beyond the far infrared. Note as well from Fig.

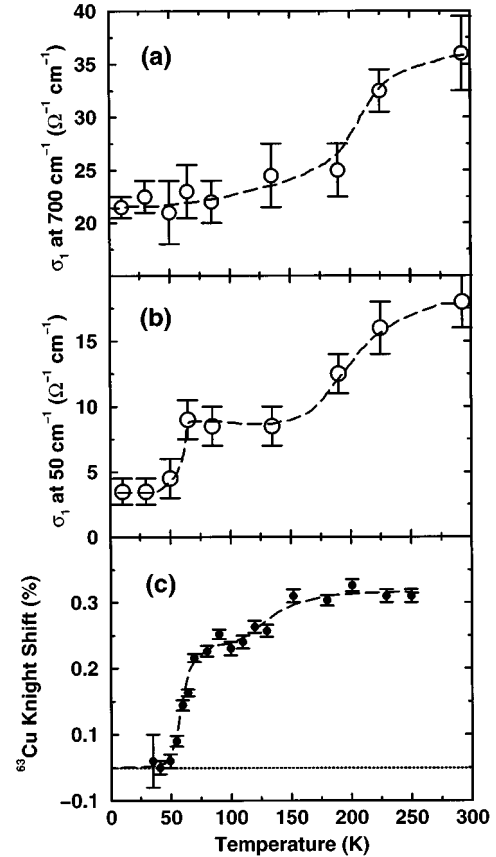


FIG. 3. Temperature dependence of the c -axis optical conductivity of underdoped $\text{Pb}_2\text{Sr}_2(\text{Y}/\text{Ca})\text{Cu}_3\text{O}_8$ measured (a) at 700 cm^{-1} , above the range of the phonons, and (b) at 50 cm^{-1} below the range of the phonons, compared (c) to that of the spin component of the ^{63}Cu NMR Knight shift. Note in both (a) and (b) the depressed conductivity below 200 K. The transfer of spectral weight to the superconducting condensate at T_c is clearly seen in the low-frequency data of (b). The temperature dependence of the NMR Knight shift echoes that of the low-frequency optical conductivity. Lines are a guide to the eye.

1 that the ab -plane dc resistivity of underdoped $\text{Pb}_2\text{Sr}_2(\text{Y}/\text{Ca})\text{Cu}_3\text{O}_8$ exhibits a pronounced change in slope between 150 and 200 K, a signature of the formation of the pseudogap.¹²

The second point to note is that the overall magnitude of the c -axis background optical conductivity of underdoped $\text{Pb}_2\text{Sr}_2(\text{Y}/\text{Ca})\text{Cu}_3\text{O}_8$ ($\approx 20\text{ }\Omega^{-1}\text{ cm}^{-1}$ near 700 cm^{-1}), while somewhat greater than that of single-layer $\text{La}_{2-x}\text{Sr}_x\text{CuO}_{4-y}$ ($\approx 10\text{ }\Omega^{-1}\text{ cm}^{-1}$ near 700 cm^{-1}),^{5,6} is half that of underdoped $\text{YBa}_2\text{Cu}_3\text{O}_{7-x}$ with $x=0.3$ ($\approx 40\text{ }\Omega^{-1}\text{ cm}^{-1}$ near 700 cm^{-1}),² similar to underdoped $\text{YBa}_2\text{Cu}_3\text{O}_{7-x}$ with $x=0.5$,² and considerably smaller than that of $\text{YBa}_2\text{Cu}_4\text{O}_8$ ($\approx 150\text{ }\Omega^{-1}\text{ cm}^{-1}$ near 650 cm^{-1}),⁴ suggesting that the appearance of a far-infrared pseudogap edge is likely not related to either the absolute value of the c -axis conductivity or to whether or not the materials are of a single- or double-layer nature.

Although the exact shape of the background conductivity of underdoped $\text{Pb}_2\text{Sr}_2(\text{Y}/\text{Ca})\text{Cu}_3\text{O}_8$ could not be unambiguously extracted, it is clear from Fig. 2 that it is decidedly non-Drude-like in the normal state, with a magnitude signifi-

cantly smaller than Mott's minimum metallic conductivity limit, indicating incoherent out-of-plane transport. This observation is consistent with *c*-axis dc-resistivity measurements which show that in underdoped crystals of $\text{Pb}_2\text{Sr}_2(\text{Y}/\text{Ca})\text{Cu}_3\text{O}_8$ the *c*-axis resistivity exhibits a semiconductinglike increase with decreasing temperature in the normal state, in contrast to optimally doped samples where the *c*-axis resistivity decreases in a metallic fashion with decreasing temperature.¹⁶

A dramatic change occurs in the optical properties of $\text{Pb}_2\text{Sr}_2(\text{Y}/\text{Ca})\text{Cu}_3\text{O}_8$ below T_c . A prominent plasma edge appears in the reflectance,³ indicating that the onset of superconductivity is accompanied by coherent interlayer charge transport. Analysis in terms of the ω^{-2} dependence of the real part of the dielectric function, ϵ_1 , of a δ function ($\Gamma \rightarrow 0$) Drude condensate yields a plasma frequency of $\omega_p = 285 \text{ cm}^{-1}$ and a London penetration depth of $5.6 \mu\text{m}$.³ The conductivity sum rule gives the spectral weight of the condensate via $\int \sigma(\Omega^{-1} \text{ cm}^{-1}) d\omega = \omega_p^2 / (8 \times 4.77 \Omega) = 2125 \Omega^{-1} \text{ cm}^{-2}$, where ω_p is in cm^{-1} and 4.77Ω is a multiplicative factor used to convert conductivity in units of $\Omega^{-1} \text{ cm}^{-1}$ to units of cm^{-1} . The quantity $2125 \Omega^{-1} \text{ cm}^{-2}$ represents the missing area between the background conductivity of the 65 and 10 K curves of Fig. 2(c).

The low-frequency optical conductivity in the superconducting state, while extremely small ($\approx 4 \Omega^{-1} \text{ cm}^{-1}$) remains finite to the lower limit of the range investigated. This is also observed in the other families of high- T_c materials. Figure 3 shows that the onset of superconductivity manifests itself on the background conductivity only in the low-frequency data which experiences a further depression, by about a factor of 2 ($5 \Omega^{-1} \text{ cm}^{-1}$), as a result of this transfer of spectral weight into the δ -function condensate at zero frequency. Concurring with the magnetization data of Fig. 1 this is found to occur at a decreased T_c of approximately 65 K. As indicated by the shaded rectangular bar in Fig. 2(c), the missing spectral weight can be accounted for by a depression of $5 \Omega^{-1} \text{ cm}^{-1}$ over a frequency range of 425 cm^{-1} , which would explain the observation that the conductivity at frequencies above 500 cm^{-1} does not appear to be affected by the onset of superconductivity. This energy scale is however considerably higher than that of $3.5kT_c \approx 160 \text{ cm}^{-1}$.

Comparison of Figs. 3(b) and 3(c) reveals that the temperature dependence of the low-frequency *c*-axis optical conductivity is similar to that of the ^{63}Cu NMR Knight shift. Both the low-frequency optical conductivity, and the spin component of the Knight shift decrease rapidly with the onset of superconductivity. Above T_c , both quantities are depressed from their high-temperature values in an intermediate-temperature regime extending from just above

T_c to approximately 150 K. This depression is interpreted to be the result of the formation of a pseudogap. A more detailed study of NMR measurements of underdoped $\text{Pb}_2\text{Sr}_2(\text{Y}/\text{Ca})\text{Cu}_3\text{O}_8$ is presented elsewhere.¹⁸ We note here, however, that a close correspondence between the temperature dependence of the *c*-axis optical conductivity and of the NMR Knight shift has also been observed for $\text{YBa}_2\text{Cu}_3\text{O}_7$ (Ref. 2) and $\text{YBa}_2\text{Cu}_4\text{O}_8$,⁴ and has been taken as evidence for an association of the pseudogap state with the opening of a gap in the spectrum of spin excitations which affects the conductivity (charge transport) via an interaction between the charge and spin excitations.¹⁹

The cumulative evidence thus points towards the existence of a pseudogap in the normal-state *c*-axis conductivity of underdoped $\text{Pb}_2\text{Sr}_2(\text{Y}/\text{Ca})\text{Cu}_3\text{O}_8$ which is characterized by a non-Drude incoherent transport, and is fully developed at a temperature of the order 150 K with a temperature dependence that is echoed in both the dc resistivity and the NMR Knight shift. The superconducting state is characterized, as it is for several other families of high- T_c compounds, by the reappearance of coherent transport as a result of a transfer of spectral weight from an energy scale considerably higher than $3.5kT_c$ into a δ -function condensate.

V. CONCLUSION

The far-infrared *c*-axis optical conductivity of underdoped $\text{Pb}_2\text{Sr}_2(\text{Y}/\text{Ca})\text{Cu}_3\text{O}_8$ has been found to be systematically depressed with decreasing temperature between 300 and 150 K, providing evidence, together with dc resistivity and NMR Knight-shift measurements, for the formation of a pseudogap in the normal state. No clear gap edge was observable suggesting that like $\text{La}_{2-x}\text{Sr}_x\text{CuO}_{4-y}$, the energy scale for the pseudogap extends into the mid-infrared, and is thus higher than that for $\text{YBa}_2\text{Cu}_4\text{O}_8$ and underdoped $\text{YBa}_2\text{Cu}_3\text{O}_{7-x}$, where it is of the order 300 cm^{-1} . Upon entry to the superconducting state coherent transport sets in, and the *c*-axis conductivity at the lowest frequencies is further depressed due to a transfer of spectral weight into the δ -function Drude condensate. The redistributed normal-state spectral weight is estimated to derive from frequencies up to approximately 425 cm^{-1} , an energy scale significantly higher than $3.5kT_c$.

ACKNOWLEDGMENTS

We are grateful to C. V. Stager for the use of the magnetometer. Optical reflectance, dc-resistivity, and magnetization measurements were carried out at McMaster University. The NMR work was done at the University of Toronto. Financial support was provided by the Natural Sciences and Engineering Research Council (NSERC) of Canada.

*Present address: Ultralife Batteries, Inc., 1350 Route 88 S., Newark, NY 14450.

¹For a review, see, D. B. Tanner and T. Timusk, in *Physical Properties of High Temperature Superconductors III*, edited by D. M. Ginsberg (World Scientific, Singapore, 1992).

²C. C. Homes, T. Timusk, R. Liang, D. A. Bonn, and W. N. Hardy, Phys. Rev. Lett. **71**, 1645 (1993); Physica C **254**, 265

(1995).

³M. Reedyk, T. Timusk, J. S. Xue, and J. E. Greedan, Phys. Rev. B **49**, 15 984 (1994).

⁴D. N. Basov, T. Timusk, B. Dabrowski, and J. D. Jorgensen, Phys. Rev. B **50**, 3511 (1994).

⁵S. Uchida, K. Tamasaku, K. Takenaka, and H. Takagi, J. Low Temp. Phys. **95**, 109 (1994); S. Uchida, K. Tamasaku, and S.

- Tajima, Phys. Rev. B **53**, 14 558 (1996).
- ⁶D. N. Basov, H. A. Mook, B. Dabrowski, and T. Timusk, Phys. Rev. B **52**, R13 141 (1995).
- ⁷For earlier work, see citations 11–19 of Ref. 3.
- ⁸Y. Iye, T. Sakakibara, T. Goto N. Miura, H. Takeya, and H. Takei, Physica C **153–155**, 26 (1988).
- ⁹M. Takigawa and D. B. Mitzi, J. Low Temp. Phys. **95**, 89 (1994); M. Takigawa, A. P. Reyes, P. C. Hammel, J. D. Thompson, R. H. Heffner, Z. Fisk, and K. C. Ott, Phys. Rev. B **43**, 247 (1991).
- ¹⁰J. W. Loram, K. A. Mirza, J. M. Wade, J. R. Cooper, and W. Y. Liang, Physica C **235–240**, 134 (1994).
- ¹¹M. Matsuda, K. Yamada, Y. Endoh, T. R. Thurston, G. Shirane, R. J. Birgeneau, M. A. Kastner, I. Tanaka, and H. Kojima, Phys. Rev. B **49**, 6958 (1994).
- ¹²T. Ito, K. Takenaka, and S. Uchida, Phys. Rev. Lett. **70**, 3995 (1993); B. Batlogg, H. Y. Hwang, H. Takagi, R. J. Cava, H. L. Kao, and J. Kwo, Physica C **235–240**, 130 (1994); B. Bucher, P. Steiner, J. Karpinski, E. Kaldis, and P. Wachter, Phys. Rev. Lett. **70**, 2012 (1993).
- ¹³D. N. Basov, R. Liang, B. Dabrowski, D. A. Bonn, W. N. Hardy, and T. Timusk, Phys. Rev. Lett. **77**, 4090 (1996).
- ¹⁴A. V. Puchkov, P. Fournier, D. N. Basov, T. Timusk, A. Kapit-ulnik, and N. N. Kolesnikov, Phys. Rev. Lett. **77**, 3212 (1996).
- ¹⁵J. S. Xue, M. Reedyk, Y. P. Lin, C. V. Stager, and J. E. Greedan, Physica C **166**, 29 (1990); J. S. Xue, M. Reedyk, A. Dabkowska, H. Dabkowska, J. E. Greedan, and C. H. Chen, J. Cryst. Growth **113**, 371 (1991).
- ¹⁶M. Reedyk, J. S. Xue, J. E. Greedan, and T. Timusk, in *Superconductivity and Its Applications*, edited by Y. H. Kao, A. E. Kaloyeros, and H. S. Kwok, AIP Conf. Proc. 251 (AIP, New York, 1992), p. 561.
- ¹⁷C. C. Homes, M. Reedyk, D. A. Crandles, and T. Timusk, Appl. Opt. **32**, 2976 (1993).
- ¹⁸Y.-W. Hsueh, B. W. Statt, M. Reedyk, T. Timusk, J. S. Xue, and J. E. Greedan, this issue, Phys. Rev. B **56**, R8511 (1997).
- ¹⁹L. D. Rotter, Z. Schlesinger, R. T. Collins, F. Holtzberg, C. Field, U. W. Welp, G. W. Crabtree, J. Z. Liu, Y. Fang, K. G. Vanderwort, and S. Fleshler, Phys. Rev. Lett. **67**, 2741 (1991).